

# Quantifying the Relationship Between Unilateral Induced Metamorphopsia and Stereopsis Impairment

Lingxian Xu, Lu Liu, Bo Yu, Ning Yang, and Huang Wu

Department of Optometry, The Second Hospital of Jilin University, Changchun, China

Correspondence: Huang Wu,  
Department of Optometry, The  
Second Hospital of Jilin University,  
No. 218, Ziqiang Street, Nangan  
District, Changchun, Jilin Province  
130041, China;  
[wuhuang@jlu.edu.cn](mailto:wuhuang@jlu.edu.cn).

**Received:** November 24, 2023

**Accepted:** March 8, 2024

**Published:** April 1, 2024

Citation: Xu L, Liu L, Yu B, Yang N,  
Wu H. Quantifying the relationship  
between unilateral induced  
metamorphopsia and stereopsis  
impairment. *Invest Ophthalmol Vis  
Sci.* 2024;65(4):2.  
<https://doi.org/10.1167/iovs.65.4.2>

**PURPOSE.** To investigate the relationship between unilateral metamorphopsia, characterized by visual distortions in one eye, and impaired stereopsis.

**METHODS.** Utilizing both near and distance measurements through advanced testing systems, including 4K smartphones and an active shutter three-dimensional system, we simulated varying degrees of unilateral metamorphopsia in 30 healthy young adults aged between 21 and 29 years. Two types of contour-based stereotest symbols, lines and squares, were developed. Distortions were classified into six distinct patterns, each further divided into eight grades of severity. Participants were tasked with identifying visual targets, and their stereothresholds were determined under different conditions of induced distortion. Stereopsis was measured within a range of 2.9 to 1.0 log arcsec, at 0.2 log arcsec intervals. Stereopsis changes under different distortion scenarios were analyzed using the generalized estimating equations, with a sequential Bonferroni adjustment applied for pairwise comparisons.

**RESULTS.** A direct and quantifiable correlation was observed between the severity of metamorphopsia and reductions in stereopsis. As the degree of visual distortion increased, notably in both frequency and amplitude, there was a corresponding decline in stereopsis. This relationship held true in both near and distance measurements of stereopsis. Statistical analyses further reinforced these findings, highlighting a significant detrimental effect of distortion components on stereoacuity.

**CONCLUSIONS.** The findings highlight the clinical significance of understanding the interplay between unilateral metamorphopsia and stereopsis. Early interventions in conditions leading to metamorphopsia might be critical to maintaining optimal stereopsis.

**Keywords:** distortion, metamorphopsia, smartphone, stereopsis

Stereopsis, or depth perception in the human visual system, results from binocular disparity as each eye sees a slightly different image due to their separation, which the brain combines into a single depth-perceived image.<sup>1</sup> Essential for accurate depth judgment and eye-hand coordination, it supports everyday activities and specialized tasks like microsurgery.<sup>2,3</sup> Impairments in stereopsis can cause deficits in visually guided hand movements,<sup>4</sup> gait changes,<sup>5</sup> or increased risk of falls and hip fractures.<sup>6,7</sup> Its complexity, extending from the retina to the visual cortex, renders it sensitive to disruptions. Disturbances within this pathway can significantly impact stereoscopic vision, leading to challenges in activities requiring precise spatial awareness and fine motor skills.<sup>8</sup>

Metamorphopsia, characterized by visual distortions where lines and flat surfaces appear curvy, wavy, or bulging, impacts patient perception significantly.<sup>9</sup> It is frequently associated with macular diseases, including age-related macular degeneration (AMD), macular hole (MH), and epiretinal membrane (ERM), which disrupt the retinal structure and photoreceptor layer.<sup>10</sup> These distortions challenge tasks requiring precision vision like reading and facial recognition.<sup>11,12</sup> Initially detected through the Amsler grid, where patients report perceived distortions in a grid of straight

lines, the reliance on subjective patient input underscores the necessity for more objective, quantitative assessment methods.<sup>9,10</sup>

Advanced tools like the Sine Amsler Charts (SACs) and Morphision offer more objective and repeatable methods for metamorphopsia assessment. SACs use sinusoidal lines allowing patients to match their distortion levels, notably in ERM cases, while Morphision employs various sine wave frequencies and amplitudes for patient feedback and quantification.<sup>13,14</sup> Additionally, M-CHARTS and preferential hyperacuity perimetry (PHP) aid in the quantification of metamorphopsia and early detection of conditions like AMD.<sup>15,16</sup>

The co-occurrence of metamorphopsia with decreased stereopsis in conditions like MH and ERM suggests a complex, underexplored relationship.<sup>17,18</sup> Metamorphopsia disrupts the spatial alignment of visual information, leading to potential differences in the images each eye relays to the brain, which could compromise stereopsis.<sup>18,19</sup> The limited direct evidence in scientific literature underscores the need for further investigation into how metamorphopsia affects stereopsis to fully understand this interaction and its clinical implications. Exploring the severity level at which metamorphopsia significantly

impacts stereopsis presents another interesting aspect of this study.

This study examines the impact of unilateral metamorphopsia on stereopsis, hypothesizing that varying levels of artificially induced visual distortions affect stereoacuity. By simulating unilateral metamorphopsia in healthy individuals using 48 distortion combinations of different types and severities, we aim to mirror unilateral metamorphopsia experiences and quantitatively evaluate stereoacuity changes.

Considering the clinical emphasis on near stereotests for conditions like AMD, ERM, and MH,<sup>17,20,21</sup> our study expands to include both near and distance stereopsis assessments. This approach acknowledges that distance and near tests probably measure different aspects of binocular vision.<sup>22</sup> Given that visual impairments' impact on stereopsis may vary between near and far conditions,<sup>23,24</sup> incorporating both measurement ranges aims to provide a comprehensive understanding of how metamorphopsia affects stereopsis. This may enhance diagnostic and therapeutic strategies for conditions involving metamorphopsia and stereopsis impairment.

## METHODS

### Participants

We recruited 30 medical students (19 females, 11 males; aged 21–29 years) with a best-corrected visual acuity of 0.0 logMAR or better and stereothresholds of 40" or better, measured by the Fly Stereo Acuity Test (Stereo Optical Company, Chicago, IL, USA). All participants provided written informed consent. This study adhered to the Declaration of Helsinki and received ethics approval from the Second Hospital of Jilin University (No. 2022-261).

### Test System

**Equipment.** Near stereopsis was assessed using a phoropter paired with two 4K smartphones (Sony Xperia XZ Premium; Sony Mobile Communications, Tokyo, Japan) with a resolution of  $3840 \times 2160$ .<sup>25,26</sup> Utilizing two 5.5 $\Delta$  base out Risley prisms, participants could fuse the images from the two smartphones into one, producing a minimum disparity of 10" (1 pixel) at a 0.65-m viewing distance on the phoropter's near-vision test rod (Topcon VT-10; Topcon Corp, Tokyo, Japan) (Fig. 1A).

Distance stereopsis was evaluated using an active shutter three-dimensional (3D) system, comprising a 3D laptop (ASUS G750Y47JX, 17.3-in. 16:9 full HD 3D [1920  $\times$  1080 120 Hz]; ASUSTEK Computer, Taipei, Taiwan) and 3D shutter glasses (Nvidia 3D Vision 2 Wireless Glasses Kit; Expressway, Santa Clara, CA, USA). Nvidia 3D Vision Photo Viewer was used to display 3D images.<sup>27</sup> The test was conducted at 4.1 m, ensuring visual angle consistency with near measurements, where 1 pixel of disparity equaled 10" (Fig. 1B).

### Test Symbols

Two stereogram types were utilized: lines and squares.

**Linear Test Symbols.** For linear units, each line measured 550 pixels in length and 44 pixels in width. Four vertical lines were aligned horizontally for the test, with a reference line placed on each side for comparison. These reference lines were identical in appearance to the four test lines but did not contain disparities. Among

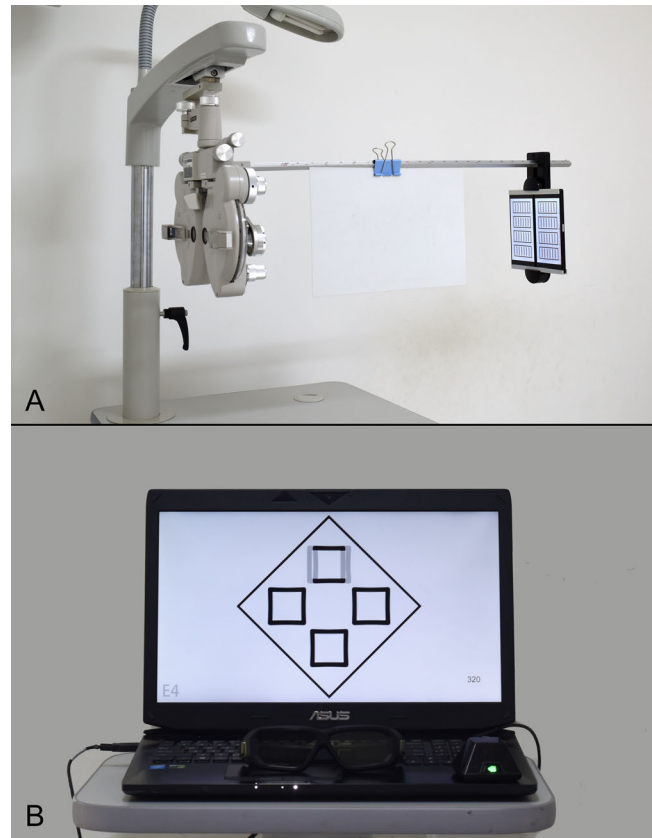


**FIGURE 1.** Photograph of the testing system. (A) Photograph showing a phoropter and two 4K smartphones used to test near stereopsis. (B) Photograph showing a 3D laptop test system used to test distance stereopsis.

the four central test lines, one was randomly selected as the stereo target, which appeared to stand out from the plane due to its crossed disparity. In each test, participants could identify the stereo target from these four options when their stereothreshold was below the set disparity (Fig. 2A).

**Square Test Symbols.** Each square in the square units measured  $218 \times 218$  pixels with line widths of 28 pixels. Among four squares arranged in a diamond configuration, one was randomly selected as the stereo target. This target square was distinguishable as it appeared to stand out from the plane due to crossed disparity. Participants could identify the stereo target from these four options when their stereothreshold was below the set disparity (Fig. 2B).

### Test Pages

**Comparison of Newly Designed and Conventional Contour Symbols.** To compare our new designs with conventional contour symbols, we devised two test pages: one for linear (Fig. 2A) and one for square symbols (Fig. 2B). Both were compared to the quantitative measurement section of the Fly Stereo Acuity Test, with disparities set at 40", 30", 20", and 10" (Fig. 2C).

**Determining the Stereothreshold.** For near measurements, each set of linear stereograms comprised three test pages. These pages featured 10 distinct disparities, specifically: 800" (2.9 log arcsec), 500" (2.7 log arcsec),

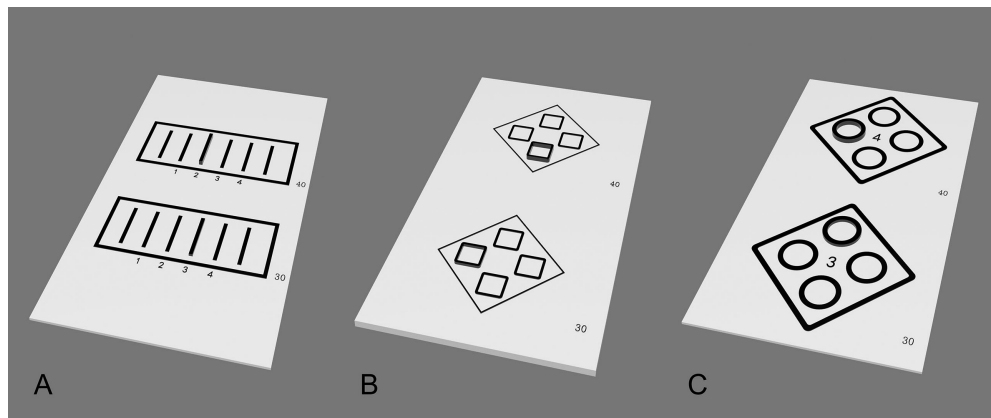


**FIGURE 2.** Simulation of perceptions generated by test images. If a patient's stereothreshold is lower than the displayed disparity, the target appeared as protruding. (A) Near measurement of stereopsis using linear symbols. The disparities of the two targets are 40'' and 30'', respectively. (B) Near measurement of stereopsis using square symbols. The disparities of the two targets are 40'' and 30'', respectively. (C) Near measurement of stereopsis using conventional contour symbols. The disparities of the target circles are 40'' and 30'', respectively.

320'' (2.5 log arcsec), 200'' (2.3 log arcsec), 120'' (2.1 log arcsec), 80'' (1.9 log arcsec), 50'' (1.7 log arcsec), 30'' (1.5 log arcsec), 20'' (1.3 log arcsec), and 10'' (1.0 log arcsec). Distance measurement with linear stereograms used 10 pages, each with one of these disparities.

Square stereograms for near tests had five pages, each with two disparities from 800'' to 10''. Square stereograms for distance tests have 10 pages, each with one of these disparities on each.

### Metamorphopsia Simulation

To simulate unilateral metamorphopsia, the test image for the right eye remained unchanged, whereas the left eye was presented with images in which the test symbols were replaced with distorted variants. We adopted six distinct patterns (A to F), each with eight severity grades (1 to 8), to represent a range of visual distortions similar to patient experiences. Specifically, patterns A to D pertained to line symbols, while E and F corresponded to square symbols. This classification takes inspiration from SACs and Morphision, which quantify metamorphopsia by comparing distortions perceived in the affected eye against simulated distortions viewed with the contralateral normal eye. Our approach, informed by these practices, aims to accurately replicate the diverse metamorphopsia encountered clinically.

**Linear Test Patterns.** Straight lines of the test symbols were substituted with sinusoidal lines of varying frequency and amplitude, creating different patterns and grades of distortion. These were generated using the LaTeX typesetting system for precise frequency and amplitude adjustments. With  $L$  representing line length, sine curve cycles were set to 0.5 (A), 1 (B), 2.5 (C), and 4 (D), equating to spatial frequencies of 0.5, 1, 2.5, and 4 cycles per  $L$ . Every pattern was categorized into eight grades, with amplitudes incrementing in 0.005  $L$  steps from 0.005 to 0.04  $L$ . To clarify, the percentage deviations for grades 1 through 8 were 0.5%, 1%, 1.5%, 2%, 2.5%, 3%, 3.5%, and 4%, respectively. Here, the amplitude signifies the maximum deviation of the wave from its center (Fig. 3).

**Square Test Patterns.** Two distortion patterns were used: cushion-like (E) and barrel-like (F), created using sinu-

soidal functions. Each square side transformed with sine curves of uniform frequency but escalating amplitudes—curves bent inward for cushion-like and outward for barrel-like distortions. Assuming  $L$  represents the side length, each curve featured 0.5 cycles, achieving a spatial frequency of 0.5 cycles per  $L$ . Similar to linear patterns, these also included eight grades with amplitudes increasing in 0.005  $L$  steps from 0.005 to 0.04  $L$  (Fig. 4).

### Test Procedure

Participant refraction was determined using standard optometry protocols, followed by appropriate refractive corrections during stereopsis measurements. For near measurements, corrective lenses were placed in the phoropter's observation aperture. For distance measurements, corrective trial lenses were provided in a trial frame as necessary. The stereopsis of all 30 participants was first tested using the newly designed and conventional contour symbols, followed by measurements of stereopsis under simulated metamorphopsia conditions.

**Comparison of Newly Designed and Conventional Contour Symbols.** The order of near and distance measurements was randomized in advance. Participants were instructed to identify the stereo target from both the Fly test pages (ranging from 40'' to 10'') and the newly designed patterns, which encompassed both line and square symbols (again, from 40'' to 10''). The minimal stereo target that could be distinguished was documented as the participant's stereothreshold. Additionally, the presentation order for the Fly, line, and square stereograms was predetermined randomly.

**Determination of Stereothreshold Under Simulated Metamorphopsia Conditions.** To emulate the experience of unilateral metamorphopsia, the right eye was presented with undistorted test pages, while the left eye viewed pages with induced distortions. The order of near and distance measurements was randomized in advance, as was the sequence for the six distinct patterns, labeled A through F. For each pattern, testing began with the highest distortion level (grade 8) and proceeded in decreasing order to grade 1. Participants were tasked with identifying the symbol (line or square) that appeared to protrude from the

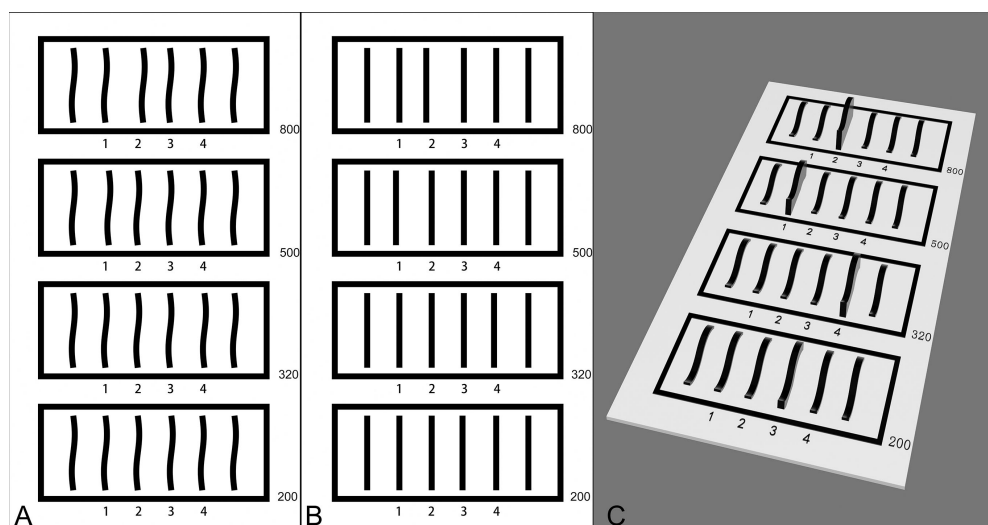


**FIGURE 3.** Legend of test page 1 with distortion of B4 for near measurement. **(A)** Image for the left eye. **(B)** Image for the right eye. **(C)** Simulation of the perceived images. The disparities of the target circles are 800'', 500'', 320'', and 200''. In the test images, the right eye image remains unchanged, while the symbols in the left eye image are replaced with sinusoidal curves having a frequency of 1 (type B) and an amplitude of 0.02 (grade 4).

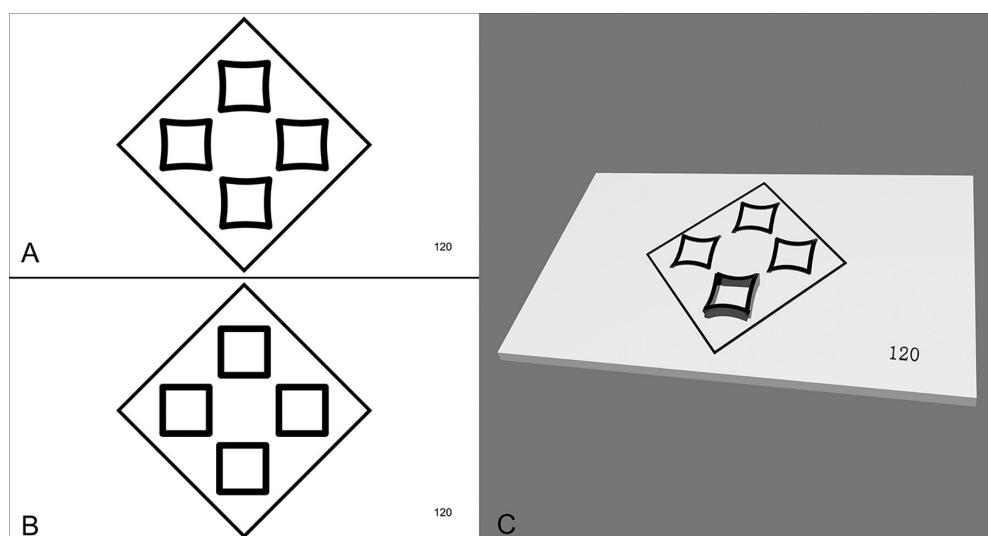


**FIGURE 4.** Legend of test page 5 with distortion of E8 for distance measurement. **(A)** Image for the left eye. **(B)** Image for the right eye. **(C)** Simulation of the perceived images. The disparity of the target square is 120''. In the test images, the right eye image remains unchanged, while the four sides of the squares in the left eye image are replaced by four identical sinusoidal curves with a frequency of 0.5 (type E) and an amplitude of 0.04 (grade 8).

plane. The evaluation started at a disparity of 800'', decreasing incrementally to 10''. The participant's final correct identification was noted as their stereothreshold. If a participant was unable to identify at the starting 800'' disparity, their stereoacuity was recorded as 1260'' (3.1 log arcsec). This methodology allowed for determining the participant's stereopsis within a range of 2.9 log arcsec (800'') to 1.0 log arcsec (10''), in increments of 0.2 log arcsec (Fig. 5).

### Statistical Analysis

Statistical analysis was performed using SPSS (version 27.0; IBM Corp, Armonk, NY, USA) and GraphPad Prism (version

8.0.1; GraphPad Software, San Diego, CA, USA). Stereopsis values were transformed to log arcsec values for analysis. The Shapiro–Wilk test assessed the normality of stereoacuity distribution. Given that the measures were not normally distributed, the Wilcoxon signed-rank test and Kendall's coefficient of concordance (Kendall's  $W$ ) were utilized to gauge the consistency between newly designed and traditional contour symbols. To address the repeated measures in our data and assess the impact of simulated distortion on stereoacuity, we utilized generalized estimating equations (GEEs) with an unstructured covariance matrix and a linear link function. A sequential Bonferroni adjustment was used for pairwise comparisons. An alpha value



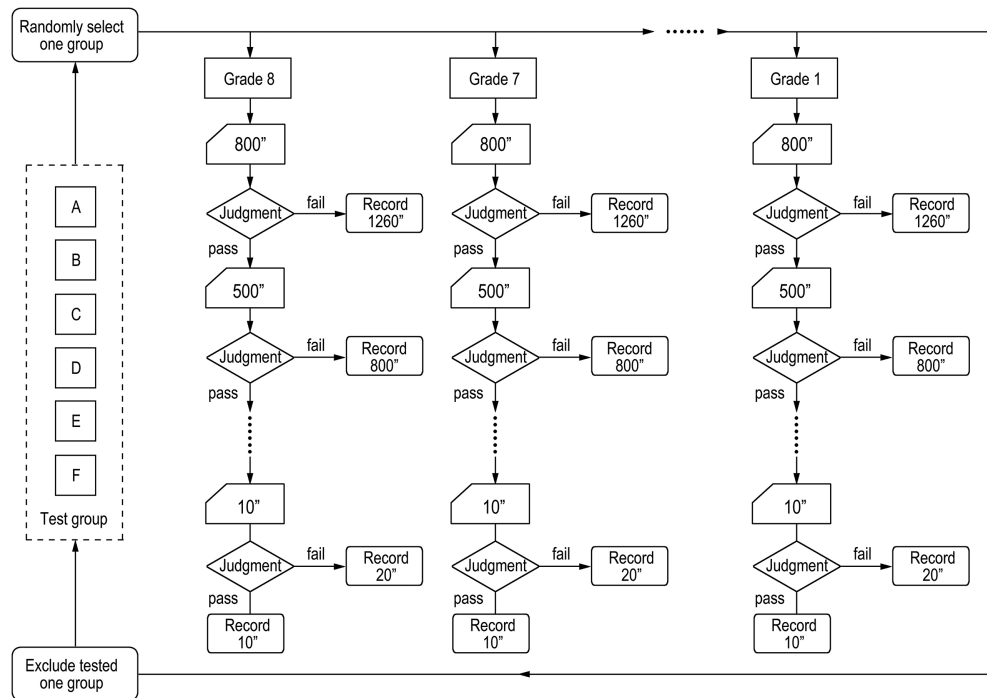


FIGURE 5. Flowchart of the test procedure for determining the threshold for near or distance stereopsis under induced distortion.

of  $\leq 0.05$  was established for all tests, denoting statistical significance.

## RESULTS

### Comparison of Newly Designed and Conventional Contour Symbols

The median values for near stereopsis, expressed in log arcsec, for the Fly, linear, and square test symbols were 1.30, 1.40, and 1.30, respectively. For distance stereopsis, the median value remained consistent at 1.30 for all three test symbols. For individual stereopsis values using the Fly, linear, and square test symbols, see Supplementary Table S1.

The Wilcoxon signed-rank test showed no significant difference between the stereothresholds measured by linear and conventional symbols ( $Z = -1.059$ ,  $P = 0.289$  for near measurement;  $Z = -0.241$ ,  $P = 0.810$  for distance measurement). Kendall's  $W$  tests indicated a significant agreement between stereothresholds measured by linear and conventional symbols (Kendall's  $W = 0.840$ ,  $P = 0.012$  for near; Kendall's  $W = 0.857$ ,  $P = 0.010$  for distance). Similar tests

for square versus conventional symbols revealed no significant difference in stereothresholds ( $Z = -1.493$ ,  $P = 0.136$  for near;  $Z = -0.206$ ,  $P = 0.837$  for distance) but showed significant agreement (Kendall's  $W = 0.903$ ,  $P = 0.005$  for near; Kendall's  $W = 0.829$ ,  $P = 0.015$  for distance).

### Determination of Stereothreshold Under Simulated Metamorphopsia Conditions

The medians and interquartile ranges (IQRs) of stereopsis values (log arcsec) for near and distance measurements are shown in Table 1 and Table 2, respectively. The stereopsis values increased with the increase of amplitude of distortion; this was observed across all six patterns in both near and distance measurements. For individual participant data, see Supplementary Table S2 for near and Supplementary Table S3 for distance measurements.

**For Patterns A, B, C, and D.** The impact of distortion's components—delineated into four frequency types (A, B, C, D) and varying amplitudes—on stereoacuity was quantitatively assessed using GEEs.

TABLE 1. Median (IQR) of Near Stereopsis Values (log arcsec) Under Varied Induced Distortion Conditions

Grades	Types					
	A	B	C	D	E	F
1	1.30 (0.50)	1.30 (0.20)	1.50 (0.20)	1.50 (0.40)	1.30 (0.50)	1.50 (0.40)
2	1.30 (0.20)	1.50 (0.20)	1.70 (0.25)	1.70 (0.40)	1.50 (0.28)	1.50 (0.40)
3	1.40 (0.20)	1.50 (0.40)	1.90 (0.45)	2.10 (0.65)	1.50 (0.40)	1.70 (0.40)
4	1.50 (0.25)	1.70 (0.20)	2.30 (0.65)	2.30 (0.60)	1.70 (0.20)	1.90 (0.25)
5	1.50 (0.40)	1.70 (0.65)	2.30 (0.40)	2.50 (0.60)	1.70 (0.20)	1.90 (0.20)
6	1.50 (0.40)	2.10 (0.80)	2.70 (0.45)	2.90 (0.65)	1.70 (0.20)	1.90 (0.05)
7	1.70 (0.60)	2.30 (0.65)	2.90 (0.40)	3.00 (0.20)	1.90 (0.40)	1.90 (0)
8	2.10 (0.65)	2.50 (0.40)	3.10 (0.20)	3.10 (0.20)	2.10 (0.60)	1.90 (0.20)

TABLE 2. Median (IQR) of Distance Stereopsis Values (log arcsec) Under Varied Induced Distortion Conditions

Grades	Types					
	A	B	C	D	E	F
1	1.30 (0.13)	1.30 (0.33)	1.30 (0.40)	1.30 (0.68)	1.30 (0.25)	1.30 (0.20)
2	1.30 (0.28)	1.50 (0.40)	1.70 (0.45)	1.70 (0.65)	1.50 (0.40)	1.50 (0.20)
3	1.30 (0.60)	1.50 (0.60)	1.70 (0.20)	1.90 (0.65)	1.50 (0.20)	1.50 (0.45)
4	1.50 (0.60)	1.70 (0.60)	1.90 (0.60)	2.10 (0.60)	1.70 (0.20)	1.90 (0.40)
5	1.70 (0.45)	1.90 (0.60)	2.30 (0.40)	2.50 (0.65)	1.70 (0)	1.90 (0.20)
6	1.80 (0.50)	1.90 (0.60)	2.50 (0.05)	2.50 (0.40)	1.70 (0.20)	2.00 (0.20)
7	1.90 (0.80)	1.90 (0.60)	2.50 (0.60)	2.70 (0.60)	1.80 (0.20)	2.10 (0.20)
8	2.10 (0.65)	2.30 (0.45)	3.10 (0.45)	3.10 (0.45)	1.80 (0.20)	2.10 (0.05)

For near measurement, GEEs revealed significant main effects for both amplitude ( $\chi^2(1) = 759.383, P < 0.001$ ) and frequency type ( $\chi^2(3) = 29.669, P < 0.001$ ). Amplitude, treated as a continuous variable, was positively associated with stereoacuity, indicating that increases in amplitude corresponded to a deterioration in stereopsis ( $B = 0.189, P < 0.001$ ). Pairwise comparisons confirmed significant differences in stereopsis among all types (all  $P \leq 0.001$ ), with type D being the most detrimental to stereoacu-

ity, followed by types C and B, while type A had the least impact. Furthermore, the interaction between type and amplitude was significant ( $\chi^2(3) = 104.442, P < 0.001$ ), illustrating that the impact of amplitude on stereoacuity varies according to frequency type. Specifically, the association between increased amplitude and poorer stereoacuity was more pronounced for types B ( $B = 0.120, P < 0.001$ ), C ( $B = 0.204, P < 0.001$ ), and D ( $B = 0.193, P < 0.001$ ) compared to type A, as depicted in Figure 6A.

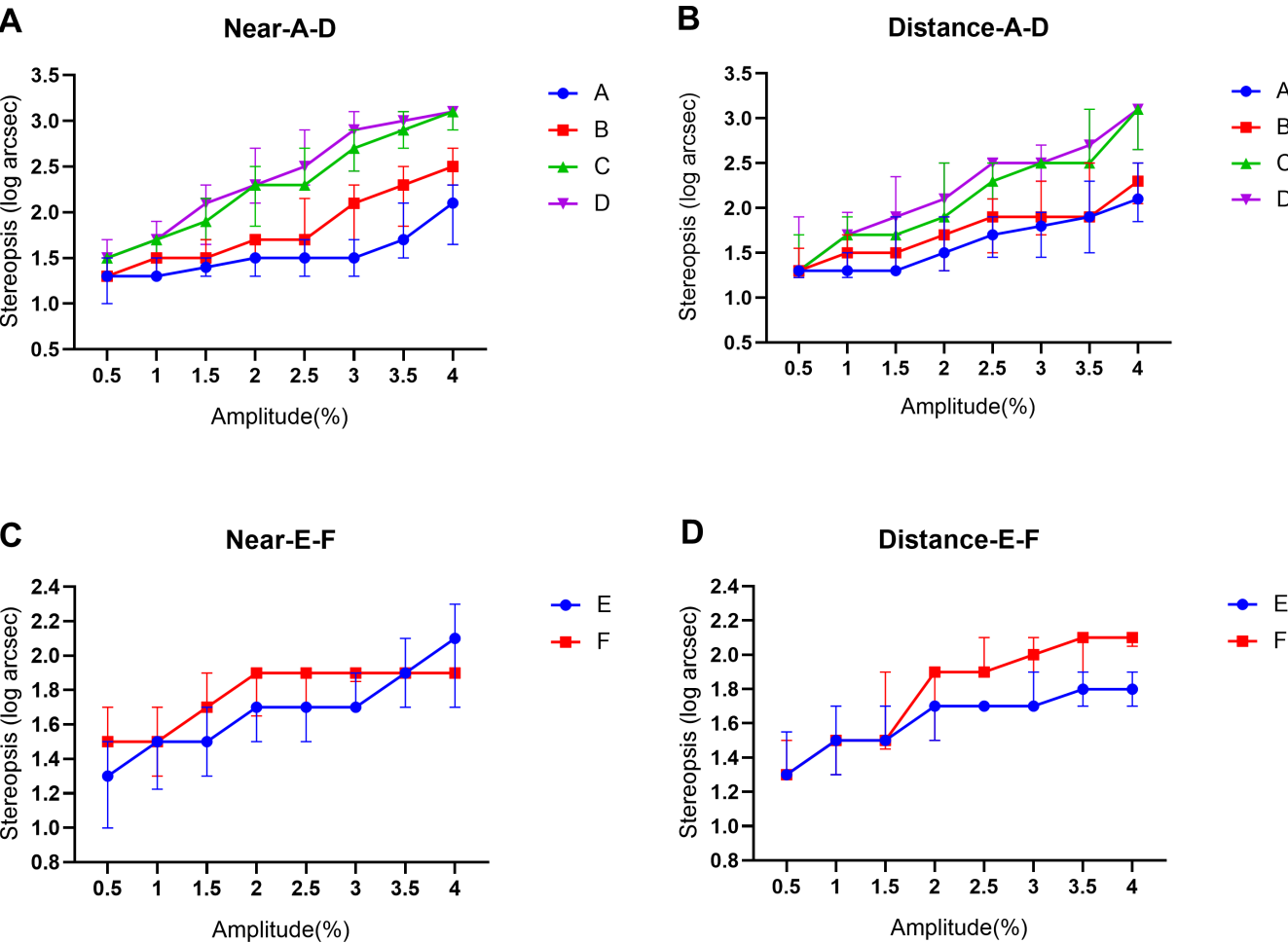


FIGURE 6. Relationship between induced distortion and stereopsis values (log arcsec). (A) Relationship between distortion of patterns A to D and near stereopsis. (B) Relationship between distortion of patterns A to D and distance stereopsis. (C) Relationship between distortion of patterns E and F and near stereopsis. (D) Relationship between distortion of patterns E and F and distance stereopsis. In these plots, the horizontal coordinate represents amplitude, described as the percentage deviation from the center, and the vertical coordinate represents the log arcsec values of stereopsis. Datapoints and error bars represent median with IQR.

For distance measurement, GEEs revealed significant main effects for both amplitude ( $\chi^2(1) = 523.805$ ,  $P < 0.001$ ) and frequency type ( $\chi^2(3) = 12.619$ ,  $P = 0.006$ ). Amplitude was positively associated with stereoacuity, indicating that increases in amplitude corresponded to a deterioration in stereopsis ( $B = 0.228$ ,  $P < 0.001$ ). Pairwise comparisons confirmed significant differences in stereopsis among all types ( $P < 0.001$  to  $P = 0.037$ ), with type D being the most detrimental to stereoacuity, followed by types C and B, with type A having the least impact. Additionally, the interaction between type and amplitude was significant ( $\chi^2(3) = 62.287$ ,  $P < 0.001$ ), denoting that the influence of amplitude on stereoacuity varies according to frequency type. Specifically, the detrimental association between increased amplitude and stereoacuity was more pronounced for types B ( $B = 0.039$ ,  $P = 0.008$ ), C ( $B = 0.160$ ,  $P < 0.001$ ), and D ( $B = 0.172$ ,  $P < 0.001$ ) compared to type A, as depicted in Figure 6B.

**For Patterns E and F.** The influence of varying amplitudes on stereoacuity within the contexts of metamorphopsia's groups E and F was analyzed using GEEs.

For near measurement, there were significant main effects of amplitude in both groups (E:  $\chi^2(1) = 148.514$ ,  $P < 0.001$ ; F:  $\chi^2(1) = 42.860$ ,  $P < 0.001$ ), with increases in amplitude consistently leading to poorer stereoacuity for both groups (E:  $B = 0.192$ ,  $P < 0.001$ ; F:  $B = 0.129$ ,  $P < 0.001$ ), as depicted in Figure 6C.

Distance measurements revealed significant main effects of amplitude in both groups (E:  $\chi^2(1) = 49.266$ ,  $P < 0.001$ ; F:  $\chi^2(1) = 162.275$ ,  $P < 0.001$ ). A rise in amplitude was consistently associated with an increased deterioration in stereopsis for both groups (E:  $B = 0.134$ ,  $P < 0.001$ ; F:  $B = 0.210$ ,  $P < 0.001$ ), as demonstrated in Figure 6D.

## DISCUSSION

In this study, line and square stereotest symbols were introduced and compared with traditional contour symbols for both near and distance vision. The results showed high concordance with conventional symbols, suggesting their potential effectiveness in stereoacuity measurement. Chosen for their sensitivity to visual distortions common in macular diseases, lines effectively detect subtle changes like waviness, while squares capture complex patterns such as cushion-like distortions.<sup>9,13,28</sup> These shapes, combined with varied frequencies and amplitudes, could effectively simulate the diverse perceptual experiences of patients with metamorphopsia, a key aspect in assessing their impact on stereopsis.

In our study, the simulation of visual distortions, encompassing six patterns and eight grades, is informed by the empirical results and methodologies of the SACs and Morphision tests. Our use of sinusoidal lines corresponds to the frequencies and amplitudes utilized in the Morphision test, aligning with clinically observed patterns of metamorphopsia. The SAC method, employed with 63 ERM patients, showed that these patients experienced metamorphopsia within five of the eight possible amplitude grades.<sup>14</sup> Similarly, the Morphision study, involving 25 patients with unilateral macular diseases, indicated that patients identified metamorphopsia corresponding to specific distortion patterns (A to E) with varied amplitudes.<sup>13</sup>

Subsequently, we explored the link between unilateral metamorphopsia and stereopsis, revealing a direct correlation: the severity of visual distortion, in both frequency and

amplitude, was closely associated with stereopsis impairment. Increased amplitude of metamorphopsia in square test symbols (E, F) aligns with impaired stereopsis in both near and distance vision. This is evident in both cushion-like (E) and barrel-like (F) distortions, with the former commonly observed in patients with MH.<sup>13,28</sup> Similarly, linear test symbols (A, B, C, D) demonstrate a rise in stereoacuity with greater frequency and amplitude of metamorphopsia, although the degree of impact varies across frequencies.

Unilateral metamorphopsia involves one eye perceiving a distorted image while the other maintains a clear view. The resulting discrepancy disrupts the normal processes of image fusion and binocular disparity, both of which are foundational to stereopsis. Consequently, the severity of visual distortion, particularly in the affected eye, directly correlates with a reduction in stereopsis. Our findings align with the understanding that greater differences in visual input between the two eyes present more significant challenges for the brain's ability to construct a reliable 3D perception.

Considerable interindividual differences in the effect of visual distortion on stereoacuity were noted, as evidenced by wider IQRs in certain testing conditions. Such findings indicate individual variability in sensitivity to induced visual distortions, emphasizing the need to consider personal reactions in clinical assessments.

The literature suggests a potential correlation between metamorphopsia and stereopsis, although definitive conclusions remain elusive.<sup>17,20,29,30</sup> Piano et al.<sup>30</sup> reported a quantitative correlation between the severity of perceptual visual distortions and poorer stereopsis among amblyopic subjects, using Frisby or preschool Randot stereotests. Similarly, research has often highlighted the co-occurrence of metamorphopsia and reduced stereopsis in retinal diseases.<sup>17,18</sup> However, studies show inconsistent results regarding a direct correlation. For example, Okamoto et al.<sup>20,31</sup> observed that metamorphopsia severity, assessed using M-CHARTS, correlated positively with TNO stereotest scores in both ERM patients and postsurgery unilateral retinal detachment patients, but this correlation was not evident with the Titmus stereotest. In contrast, studies on MH and branch retinal vein occlusion patients, along with additional research on ERM surgeries, did not find a significant correlation between metamorphopsia severity and stereoacuity.<sup>17,29,32</sup> The stereotests employed in these studies primarily focused on near vision, lacking assessments for distance stereopsis. Our research contributes quantitative evidence supporting the correlation between metamorphopsia and stereopsis impairment across both near and distance vision, indicating that metamorphopsia significantly impacts the ability for depth perception.

Aniseikonia, involving perceived image size differences between eyes, is intricately linked with metamorphopsia.<sup>33</sup> Aniseikonia relates to photoreceptor density variations, while metamorphopsia involves their distribution; both are rooted in abnormal photoreceptor alignment.<sup>34,35</sup> Studies show a connection between aniseikonia and metamorphopsia, both associated with retinal displacement and thickening of the inner nuclear layer.<sup>34,36–40</sup> Notably, studies indicate a significant correlation between increased aniseikonia and declined stereopsis.<sup>20,41</sup> Aniseikonia and metamorphopsia, by creating a mismatch in the images perceived by each eye, disrupt the brain's ability to process a unified 3D image. The

intricate mechanisms underlying these relationships remain an area of ongoing exploration.

In exploring the severity threshold of metamorphopsia that leads to significant stereopsis impairment, understanding test–retest reliability for conventional stereotests is essential. Previous studies<sup>42,43</sup> suggest that a change of at least two octaves, equivalent to a 0.6 log arcsec alteration in stereoacuity, is commonly used to delineate significant changes beyond the test–retest variability observed in clinical stereotests. With our study's baseline at 1.3 log arcsec (20"), declines beyond 1.9 log arcsec (80") are deemed significant. The data show such notable deterioration mainly in the higher grades of patterns C and D, suggesting a substantial degree of metamorphopsia is needed for a significant stereoacuity change. Thus, early detection and management of metamorphopsia may greatly mitigate its effect on stereopsis.

As metamorphopsia progresses, individuals may face challenges in activities requiring binocular stereovision, such as grasping and other motor skills tasks.<sup>3,44</sup> This can be underscored by the fact that individuals may experience metamorphopsia in daily life, even when clinical measurements do not indicate significant distortions.<sup>45</sup> With the increasing prevalence of retinal diseases like AMD and ERM, which often lead to metamorphopsia, fully understanding its clinical impact is crucial.<sup>46–48</sup>

This study has several limitations. The use of contour-based stereoscopic test symbols might introduce monocular cues, potentially affecting the measured stereopsis. The simulated distortion scenarios might not capture the full range of metamorphopsia experienced clinically. Moreover, the potential impact of top-down influences on the perception of metamorphopsia was not explored.<sup>49</sup> The age group of our young adult cohort also diverges from the typical elderly demographic affected by AMD, ERM, and others, which could limit the generalizability of our findings.<sup>46,50–52</sup> Furthermore, given that clinical stereotests are not interchangeable,<sup>53</sup> the relationship between metamorphopsia and stereoacuity observed in this study might differ from those observed in other tests. Future research involving broader age groups and various stereotests may provide additional insights.

## CONCLUSIONS

Our study demonstrated a direct correlation between unilateral metamorphopsia severity and impaired stereopsis. As the degree of visual distortion increased in one eye, stereopsis correspondingly declined. These findings highlight the need for early intervention in metamorphopsia to maintain stereopsis and underscore the clinical importance of thorough assessments and customized treatments for affected patients.

## Acknowledgments

The authors thank Marta Ugarte, Manchester Royal Eye Hospital, for providing invaluable assistance and the Morphision method, which significantly contributed to this research.

Supported by the Jilin Provincial Science & Technology Department, China (No. 20230203100SF).

Disclosure: **L. Xu**, None; **L. Liu**, None; **B. Yu**, None; **N. Yang**, None; **H. Wu**, None

## References

- Parker AJ. Binocular depth perception and the cerebral cortex. *Nat Rev Neurosci*. 2007;8:379–391.
- Dutton J, Watkins A, Henderson J, et al. Influence of stereopsis on the ability to perform simulated microsurgery. *J Cataract Refract Surg*. 2020;46:549–554.
- O'Connor AR, Birch EE, Anderson S, Draper H. The functional significance of stereopsis. *Invest Ophthalmol Vis Sci*. 2010;51:2019–2023.
- Melmoth DR, Finlay AL, Morgan MJ, Grant S. Grasping deficits and adaptations in adults with stereo vision losses. *Invest Ophthalmol Vis Sci*. 2009;50:3711–3720.
- Buckley JG, Panesar GK, MacLellan MJ, Pacey IE, Barrett BT. Changes to control of adaptive gait in individuals with long-standing reduced stereoacuity. *Invest Ophthalmol Vis Sci*. 2010;51:2487–2495.
- Ivers RQ, Norton R, Cumming RG, Butler M, Campbell AJ. Visual impairment and risk of hip fracture. *Am J Epidemiol*. 2000;152:633–639.
- Dhital A, Pey T, Stanford MR. Visual loss and falls: a review. *Eye (Lond)*. 2010;24:1437–1446.
- Levi DM. Learning to see in depth. *Vision Res*. 2022; 200:108082.
- Amsler M. Earliest symptoms of diseases of the macula. *Br J Ophthalmol*. 1953;37:521–537.
- Simunovic MP. Metamorphopsia and its quantification. *Retina*. 2015;35:1285–1291.
- Dear M, Harrison WJ. The influence of visual distortion on face recognition. *Cortex*. 2022;146:238–249.
- van de Put MA, Vehof J, Hooymans JM, Los LI. Postoperative metamorphopsia in macula-off rhegmatogenous retinal detachment: associations with visual function, vision related quality of life, and optical coherence tomography findings. *PLoS One*. 2015;10:e0120543.
- Ugarte M, Shunmugam M, Laidlaw DA, Williamson TH. Morphision: a method for subjective evaluation of metamorphopsia in patients with unilateral macular pathology (i.e., full thickness macular hole and epiretinal membrane). *Indian J Ophthalmol*. 2013;61:653–658.
- Bouwens MD, Van Meurs JC. Sine Amsler Charts: a new method for the follow-up of metamorphopsia in patients undergoing macular pucker surgery. *Graefes Arch Clin Exp Ophthalmol*. 2003;241:89–93.
- Arimura E, Matsumoto C, Nomoto H, et al. Correlations between M-CHARTS and PHP findings and subjective perception of metamorphopsia in patients with macular diseases. *Invest Ophthalmol Vis Sci*. 2011;52:128–135.
- Nowomiejska K, Oleszczuk A, Brzozowska A, et al. M-charts as a tool for quantifying metamorphopsia in age-related macular degeneration treated with the bevacizumab injections. *BMC Ophthalmol*. 2013;13:13.
- Okamoto F, Morikawa S, Moriya Y, et al. Vision-related parameters that affect stereopsis in patients with macular hole. *Sci Rep*. 2020;10:2805.
- Iuliano L, Fogliato G, Gorgoni F, Corbelli E, Bandello F, Codenotti M. Idiopathic epiretinal membrane surgery: safety, efficacy and patient related outcomes. *Clin Ophthalmol*. 2019;13:1253–1265.
- Midena E, Vujosevic S. Metamorphopsia: an overlooked visual symptom. *Ophthalmic Res*. 2015;55:26–36.
- Okamoto F, Morikawa S, Sugiura Y, Hoshi S, Hiraoka T, Oshika T. Preoperative aniseikonia is a prognostic factor for postoperative stereopsis in patients with unilateral epiretinal membrane. *Graefes Arch Clin Exp Ophthalmol*. 2020;258:743–749.
- Cao KY, Markowitz SN. Residual stereopsis in age-related macular degeneration patients and its impact on vision-related abilities: a pilot study. *J Optom*. 2014;7:100–105.



22. Yildirim C, Altinsoy HI, Yakut E. Distance stereoacuity norms for the mentor B-VAT II-SG video acuity tester in young children and young adults. *J Aapos*. 1998;2:26–32.
23. Stathacopoulos RA, Rosenbaum AL, Zanon D, et al. Distance stereoacuity. Assessing control in intermittent exotropia. *Ophthalmology*. 1993;100:495–500.
24. Seki Y, Wakayama A, Takahashi R, et al. Influence of test distance on stereoacuity in intermittent exotropia. *Strabismus*. 2017;25:12–16.
25. Wu H, Liu S, Wang R. Stereoacuity measurement using a phoropter combined with two 4K smartphones. *Clin Exp Optom*. 2018;101:272–275.
26. Zhao L, Wu H. The effect of dot size in random-dot stereograms on the results of stereoacuity measurements. *BMC Ophthalmol*. 2020;20:253.
27. Wu H, Jin H, Sun Y, et al. Evaluating stereoacuity with 3D shutter glasses technology. *BMC Ophthalmol*. 2016;16:45.
28. Saito Y, Hirata Y, Hayashi A, Fujikado T, Ohji M, Tano Y. The visual performance and metamorphopsia of patients with macular holes. *Arch Ophthalmol*. 2000;118:41–46.
29. Morikawa S, Okamoto F, Murakami T, Sugiura Y, Hiraoka T, Oshika T. Visual functions affecting stereopsis in patients with branch retinal vein occlusion. *Eye (Lond)*. 2022;36:457–462.
30. Piano ME, Bex PJ, Simmers AJ. Perceptual visual distortions in adult amblyopia and their relationship to clinical features. *Invest Ophthalmol Vis Sci*. 2015;56:5533–5542.
31. Okamoto F, Murakami T, Morikawa S, Sugiura Y, Hiraoka T, Oshika T. Vision-related parameters affecting stereopsis after retinal detachment surgery. *J Clin Med*. 2023;12:1527.
32. Krarup T, Nisted I, Christensen U, Kiilgaard JF, la Cour M. Monocular and binocular end-points after epiretinal membrane surgery and their correlation to patient-reported outcomes. *Acta Ophthalmol*. 2020;98:716–725.
33. Rutstein RP, Currie DC. Topical review: retinally induced aniseikonia. *Optom Vis Sci*. 2019;96:780–789.
34. Ichikawa Y, Imamura Y, Ishida M. Inner nuclear layer thickness, a biomarker of metamorphopsia in epiretinal membrane, correlates with tangential retinal displacement. *Am J Ophthalmol*. 2018;193:20–27.
35. Takabatake M, Higashide T, Udagawa S, Sugiyama K. Postoperative changes and prognostic factors of visual acuity, metamorphopsia, and aniseikonia after vitrectomy for epiretinal membrane. *Retina*. 2018;38:2118–2127.
36. Ichikawa Y, Imamura Y, Ishida M. Metamorphopsia and tangential retinal displacement after epiretinal membrane surgery. *Retina*. 2017;37:673–679.
37. Ichikawa Y, Imamura Y, Ishida M. Associations of aniseikonia with metamorphopsia and retinal displacements after epiretinal membrane surgery. *Eye (Lond)*. 2018;32:400–405.
38. Moon BG, Yang YS, Chung H, Sohn J. Correlation between macular microstructures and aniseikonia after idiopathic epiretinal membrane removal. *Retina*. 2020;40:1160–1168.
39. Okamoto F, Sugiura Y, Okamoto Y, Hiraoka T, Oshika T. Inner nuclear layer thickness as a prognostic factor for metamorphopsia after epiretinal membrane surgery. *Retina*. 2015;35:2107–2114.
40. Okamoto F, Sugiura Y, Okamoto Y, Hiraoka T, Oshika T. Associations between metamorphopsia and foveal microstructure in patients with epiretinal membrane. *Invest Ophthalmol Vis Sci*. 2012;53:6770–6775.
41. Atchison DA, Lee J, Lu J, et al. Effects of simulated anisometropia and aniseikonia on stereopsis. *Ophthalmic Physiol Opt*. 2020;40:323–332.
42. Tsirlin I, Colpa L, Goltz HC, Wong AM. Behavioral training as new treatment for adult amblyopia: a meta-analysis and systematic review. *Invest Ophthalmol Vis Sci*. 2015;56:4061–4075.
43. Adams WE, Leske DA, Hatt SR, Holmes JM. Defining real change in measures of stereoacuity. *Ophthalmology*. 2009;116:281–285.
44. Verghese P, Tyson TL, Ghahghaei S, Fletcher DC. Depth perception and grasp in central field loss. *Invest Ophthalmol Vis Sci*. 2016;57:1476–1487.
45. Patel PJ, Steel DH, Hirneiß C, Brazier J, Aly A, Lescrauwaet B. Patient-reported prevalence of metamorphopsia and predictors of vision-related quality of life in vitreomacular traction: a prospective, multi-centre study. *Eye (Lond)*. 2019;33:435–444.
46. Rein DB, Wittenborn JS, Burke-Conte Z, et al. Prevalence of age-related macular degeneration in the US in 2019. *JAMA Ophthalmol*. 2022;140:1202–1208.
47. Li JQ, Welchowski T, Schmid M, Mauschitz MM, Holz FG, Finger RP. Prevalence and incidence of age-related macular degeneration in Europe: a systematic review and meta-analysis. *Br J Ophthalmol*. 2020;104:1077–1084.
48. Cheung N, Tan SP, Lee SY, et al. Prevalence and risk factors for epiretinal membrane: the Singapore Epidemiology of Eye Disease study. *Br J Ophthalmol*. 2017;101:371–376.
49. Wiecek E, Lashkari K, Dakin SC, Bex P. Novel quantitative assessment of metamorphopsia in maculopathy. *Invest Ophthalmol Vis Sci*. 2014;56:494–504.
50. Zhu XB, Yang MC, Wang YX, et al. Prevalence and risk factors of epiretinal membranes in a Chinese population: the Kailuan Eye Study. *Invest Ophthalmol Vis Sci*. 2020;61:37.
51. Cho SC, Park SJ, Byun SJ, Woo SJ, Park KH. Five-year nationwide incidence of macular hole requiring surgery in Korea. *Br J Ophthalmol*. 2019;103:1619–1623.
52. Zaroff CM, Knutelska M, Frumkes TE. Variation in stereoacuity: normative description, fixation disparity, and the roles of aging and gender. *Invest Ophthalmol Vis Sci*. 2003;44:891–900.
53. Leske DA, Birch EE, Holmes JM. Real depth vs Randot stereotests. *Am J Ophthalmol*. 2006;142:699–701.